Materials Research. 2014; 17(3): 603-611
DOI: http://dx.doi.org/10.1590/S1516-14392014005000051

Evaluation of a 7050-TAF Aluminum Alloy Submitted to Creep Age Forming

***Paulo Roberto Costa Junior*[a]*, *Carlos de Moura Neto*[a], *Darrell A. Wade*[b]**

[a]*Instituto Tecnológico de Aeronáutica – ITA, Praça Marechal Eduardo Gomes, 50, CEP 12228-900, São José dos Campos, SP, Brazil*
[b]*Spirit Aerosystems Inc., 3365 S Oliver St, Wichita, KS 67210, USA*

Received: June 19, 2013; Revised: January 21, 2014

CAF process combines creep and precipitation hardening which are highly dependent on time and temperature. The aging cycle relax the stresses induced during the loading phase. At the end of the process stress relaxation induces shape changes in the part but significant spring back is observed (about 70%). Usually CAF cycles for 7XXX alloys use times around 20 h and temperatures in the range of 120°C to 190°C. In the present work CAF tests were performed using the alloy 7050 in an intermediate condition named Temper to Age Forming (TAF). Using the alloy 7050-TAF resulted in significant process time reduction. From TAF temper, only 8 hours are necessary to achieve properties comparable to T74. Coupons were submitted to CAF in two levels of initial stress, 190 MPa and 290 MPa, resulting in spring back values of 70% and 60 % respectively. In addition, constant load creep tests were performed in the same stress levels and time of CAF tests to find the creep strain values. Creep tests performed under 190 MPa resulted in strain values around 0,1% after 8 h. On the other hand creep tests performed under 290 MPa failed after 7 h with creep strain values of 1,7%. Results obtained are close to that found in previous studies and it is possible to conclude that the use of alloy 7050 in TAF condition allows CAF to be done in 8 hours, since the initial stress is lower than 290 MPa.

Keywords: *creep age forming, temper to age forming, 7050 alloy*

1. Introduction

Creep Age Forming (CAF) is a process used to manufacture wing skin panels. Some examples of CAF applications include the B1B and Hawk bombers, the executive jet Gufstream G-IV and the commercial Airbus jets A330 and A340, as well as the A380[1-5].

CAF process combines forming and heat treatment and two metallurgical phenomena, creep and precipitation hardening, are the driving force for this process. Both phenomena are highly dependent on time and temperature which ate related to the heat treatment parameters of the alloy used[6].

In the CAF process, as shown in Figure 1[4], the part to be formed is forced against a tool which has a desired curvature, through clamping mechanisms or vacuum-bagging autoclave techniques. In this first step, the forces imposed are below the yielding limit of the material. Subsequent heating starts a stress-induced deformation process that allows the material to simultaneously relax these external forces through creep mechanisms and to age by precipitation hardening. The creep mechanism introduces some permanent deformation in the material. At the final stage, the part is cooled and, as the external load is removed, part of the contour is lost due to the spring back. The magnitude of the spring back is considerable, reaching about 40 up to 70% of the imposed initial curvature[7]. Spring back occurs because the holding (ageing) time, which is required to achieve proper mechanical properties, is not sufficient to fully fix the shape of the component. However, the final aged component has lower residual stresses[4,8,9] compared to structures formed by conventional forming processes such as roll forming, brake forming, shot peening or stretch forming.

Stress relaxation is observed when the material is exposed to elevated temperatures during a period of time. Stress–strain-time relations during the basic CAF forming mechanism are shown in Figure 2. Figure 2a shows the stress redistribution between initial loading and after ageing for a simple single plane bending condition. Figures 2b-d show the corresponding stress-relaxation, creep curve and the stress–strain relationship during the CAF process.

The stress relaxation (Figure 2d) may be due to the thermally activated diffusion and/or dislocation recovery and/or creep. The stress level (below yield stress) in the work-piece reduces from σ_1 to σ_2, even though the total strain, ε_T, remains constant throughout the period of ageing. The amount of inelastic strain, ε_{in}, is responsible for shaping the part. It is believed that both thermally activated stress relaxation and creep take place during the ageing[5].

The amount of relaxation is proportional to the initial stresses induced in the beginning of the process. As reported in a previous work[10] for 7475 alloy, only minor permanent shape changes can be obtained if the initial stress is less than 30 % of σ_y. As shown in Figure 3 the amount of relaxation, at same temperature, reduces when the initial stress is reduced.

Unlike other metal forming techniques, where elastic–plastic deformation of material is dominant, the

*e-mail: paulo.costajr@gmail.com

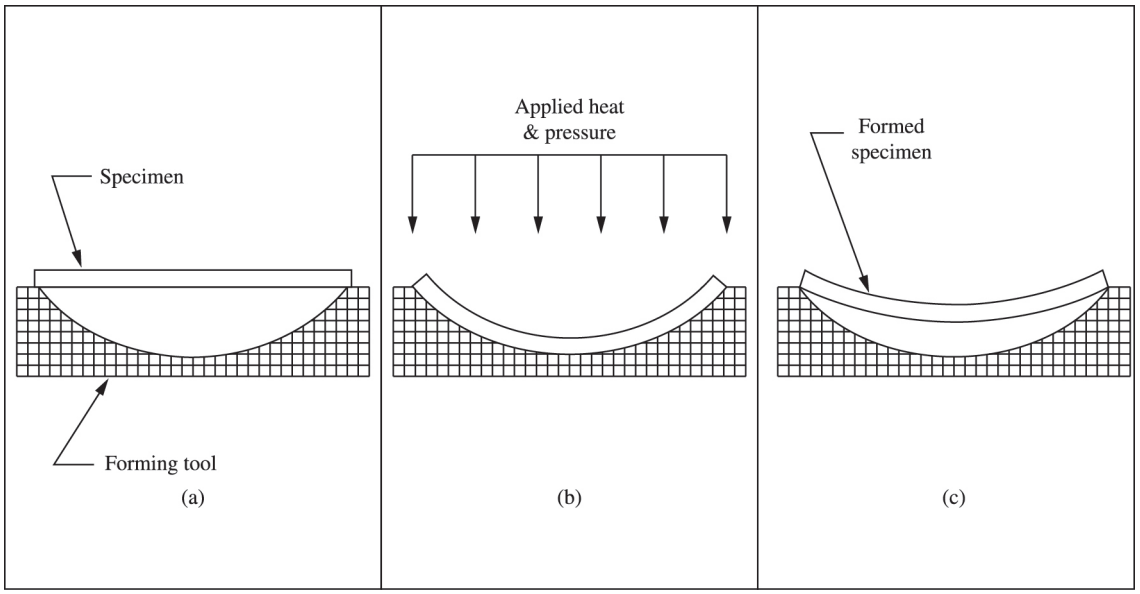

Figure 1. (a) Flat specimen prior to age forming; (b) Specimen reconfigured to assume radius; (c) Dimensionally stable, age formed specimen after experiencing springback[4].

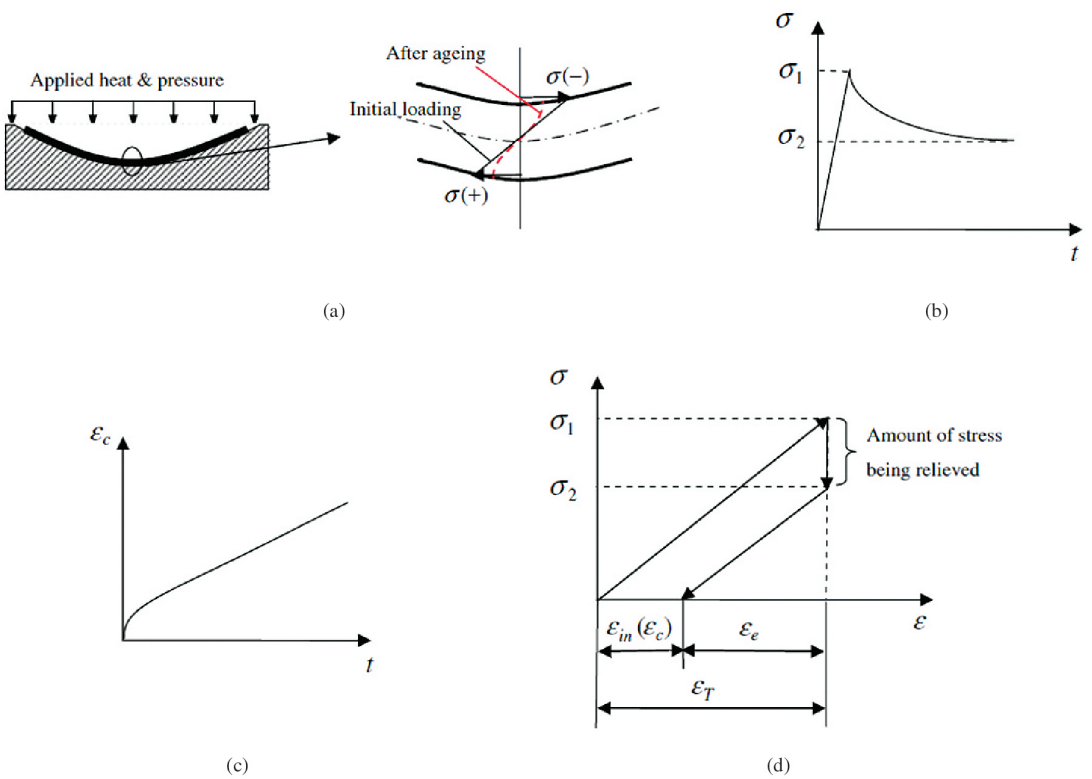

Figure 2. Forming mechanism of CAF under simple bending: (a) CAF under simple bending and stress distribution through thickness; (b) Stress relaxation - σ_1 initial stress and σ_2 threshold stress ; (c) Creep deformation; (d) Stress relaxation that occurs during CAF - σ_1 initial stress and σ_2 threshold stress[5].

'ageing–creep' deformation takes place at low stress level and the amount of plastic deformation is directly related to ageing time and temperature[7]. Furthermore, the material behavior related to age forming is more complicated than the conventional creep/stress relaxation behavior due to the precipitation hardening, which takes place simultaneously with forming process, enhances the material but decreases the creep rates. For example, the yield strength of the

material increases up to 15-25% due to ageing heat treatment[1]. Referring to the two creep curves plotted in Figure 4, the pre-aged material is stronger; exhibits little creep deformation and settles in secondary (steady) creep stage. Meanwhile, the as-quenched material, which is used in industrial age forming, shows more creep deformations and a great deal of hardening, i.e. more creep strains are developed and primary creep period is longer. This kind of 'primary creep' behavior is important since it introduces more of creep (plastic) deformation to retain the shape of component after forming[1].

Preliminary CAF studies using 7XXX alloys, which are the most common for industrial applications, report cycles with temperature in the range of 120°C to 160°C and times around 20 hours. Furthermore the alloys studied were in the solid solution condition or in the initial stage of the ageing. Spring back values around 80% were found for 7055 alloy[11] and around 70% for 7449 alloy[9]. Another work[6] that evaluates the CAF of an integrated panel machined from a 7475 alloy, report spring back values varying from 55% to 87%, depending on the section observed.

In this context, where CAF is usually done with times around 20 hours, this work presents the alloy 7050 in an intermediate temper condition called Temper to Age Forming (TAF). TAF temper is obtained when only the first step of the artificial ageing heat treatment is performed[12]. According to AMS 2770[13] the total time for AA7050

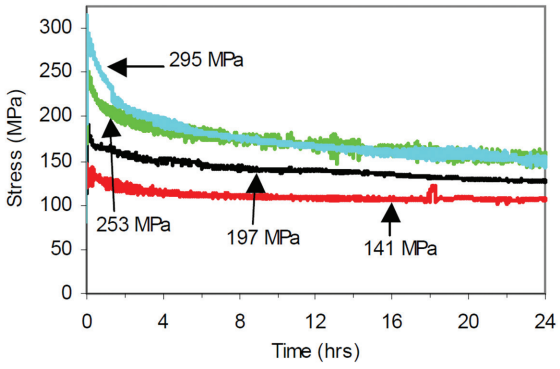

Figure 3. Example of the effect of initial stress level on the creep-relaxation behavior of 7475, during age-forming using a 2nd stage temperature of 160°C[10].

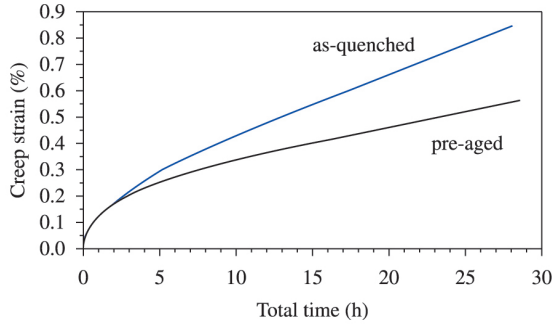

Figure 4. Comparison of creep curves for an as-quenched and a pre-aged AA7010 at 150°C[11].

artificial aging is 16 hours (8 hours for each stage). As the material is supplied in this temper condition the total time available for CAF is 8 hours which result in a reduction of 50% in CAF cycle. However, as stated before, the material strength was increased and it is necessary to perform tests in order to evaluate if the remaining time for CAF is enough to provide the creep deformation necessary to form a component. CAF tests and creep tests were performed in order to evaluate spring back values as well as creep characteristics.

2. Experimental

2.1. *Material*

The material used is an AA7050 alloy plate. Its base specification is an AMS 4050[14] with modifications in the heat treatment to obtain an intermediate temper condition denominated Temper to Age Forming (TAF)**.** Material in TAF temper was produced by the material supplier using the AMS 2770[13] heat treatment parameters to obtain T74 temper as reference. In order to verify the alloy composition, chemical analysis was performed and Table 1 presents the results.

2.2. *Tensile Tests*

Tensile tests in rolling and perpendicular to rolling directions were performed at room and elevated temperatures. The elevated temperature is the process temperature used in CAF.

The coupons used for tensile tests were machined from a 25,4 mm plate of AA7050 according to ASTM E8[15] specification. An universal testing machine from EMIC - model DL10000 (100 kN) - was used. Tensile tests were performed at a constant crosshead speed of 2 mm/min to determine mechanical properties. Yield stress and Young modulus are the main values because will be used to calculate initial stresses involved during loading phase of CAF process and the pressure necessary to push the part against the CAF tool surface.

2.3. *Creep age forming tests*

Coupons used for CAF tests measuring 400 mm x 70 mm x 10 mm and 400 mm x 70 mm x 15 mm (length x width x thickness) were machined from the center of a 25,4 mm plate of AA7050-TAF. The tool used for CAF tests was manufactured in steel and has a curved surface with a constant radius (1.600 mm). Creep Age Forming tests in rolling and perpendicular to rolling directions were performed. Figure 5 illustrates the CAF process sequence. Vacuum bag autoclave technique was used to load the coupon in the tool and two type J thermocouples were used to verify temperature during the process. Time and temperature based on AMS2770[13] parameters to obtain T74

Table 1. Chemical composition for AA7050 alloy (wt%).

Al	Zn	Mg	Cu	Fe	Si	other
Bal.	6.247	2.143	2.231	0.049	0.033	0.150

(a) (b) (c)

Figure 5. Sequence of CAF process: a) and b) vacuum bagging, c) autoclave loading.

temper, with small changes, were used in order to get the best performance for the alloy AA7050 in TAF condition.

Coupons dimensions, tool radius and E values at process temperature are known. Thus initial stresses and strains can be calculated using Equation 1 to 3. As σ_y is also known, it is possible to verify if CAF process is running under elastic conditions.

$$\varepsilon_T = \frac{(c_T - c_0)}{c_0} \quad (1)$$

$$c_T = m \times \left(r + h/2\right) \quad (2)$$

$$\sigma = E \times \varepsilon \quad (3)$$

Strain "ε_T" is calculated using Equation 1. The term "c_0" is the length of neutral line (or length of the coupon) and the term "c_T" is the length of the arc formed when the coupon is pushed against the tool surface. Equation 2 is used to calculate "c_T", where "r" is the tool radius, "h" is the coupon thickness and "m" is the angle formed by the arc "c_T" and the center of the circumference as shown in Figure 6. Equation 3 is used to calculate initial stresses "σ" involved.

Coupons were positioned in the tool using the vacuum bag technique and then creep age forming was performed in an autoclave with pressure of 0.70 MPa (100 psi). Figure 7 illustrates the load condition when the coupon is pushed against the tool surface. Equations 4 to 8 can be used to calculate necessary force to completely push the coupon against the tool surface.

In Equation 4 "σ" is the initial stress, "M_f" is flexural momentum, "I" is the inertia momentum and "y" = h/2 where "h" is the coupon thickness.

$$\sigma = \frac{M_f}{I} y \quad (4)$$

The term "c_0" in Equation 5 is the length of neutral line (or length of coupon) and "F" is the force to be calculated.

$$M_f = F\left(\frac{c_0}{2}\right) \quad (5)$$

$$y = \frac{h}{2} \quad (6)$$

The term "b" in Equation 7 is the coupon width.

$$I = \frac{bh^3}{12} \quad (7)$$

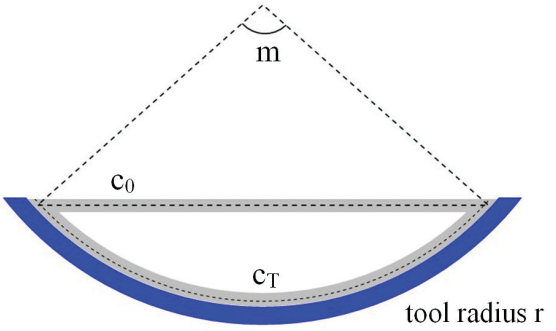

Figure 6. Sketch showing coupon over the tool: c_0 flat, c_T completely loaded in the tool surface.

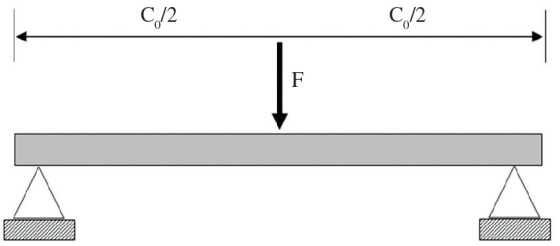

Figure 7. Sketch of the load condition when pushing the coupon against the tool surface.

$$F = \frac{\left(\sigma b h^2\right)}{3c_0} \quad (8)$$

In order to verify if the autoclave pressure provides the force enough to push the coupon against the tool, Equation 9 is used, where "σ_a" = 0.7 MPa (autoclave pressure) and "A" is the area of the coupon submitted to the pressure (not the cross section).

$$\sigma_a = \frac{F}{A} \quad (9)$$

At the end of CAF cycle the coupon is removed from the autoclave and unloaded from the tool. At this time, with no pressure acting the coupon will spring back to its final shape (or final radius) and will be measured. Deflection measurements "f" are made with the coupon in a flat table

Using the deflection values, the coupons length "L" and Equation 10 the forming radii "R_f" were calculated for every

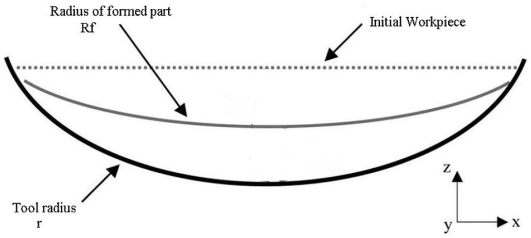

Figure 8. Spring back representation of CAF process - adapted from[10].

coupon. With the radii values, thickness "h" and Equation 11 the strain after CAF "ε_{CAF}" can be calculated.

$$R_f = \frac{\left[\left(L/2\right)^2 + (f)^2\right]}{2f} \tag{10}$$

$$\varepsilon_{CAF} = \left(\frac{h/2}{R_f - h/2}\right) \tag{11}$$

One of the most important characteristics related to CAF process is the spring back "SB%" which is represented in Figure 8 and can be calculated using Equation 12.

$$SB(\%) = \left[1 - \left(\frac{r}{R_f}\right)\right] \times 100 \tag{12}$$

2.4. *Creep Tests*

Constant load creep tests in rolling and perpendicular to rolling directions were performed at elevated temperature. Elevated temperature is the temperature used in CAF process. Time and temperature used were based on AMS2770[13] parameters required to obtain T74 temper.

Two stresses levels were used (193 MPa and 290 MPa) in order to reproduce the stress level of the CAF coupons (item 2.3) when loaded in the tool surface. A lever arm creep test system from Applied Test System (ATS) was used. The oven was modified in order to accommodate the non standard coupon. A laser extensometer from Epsilon Technology Corp (model LE05 with measurement range of 8 to 127 mm) was used to acquire strain values. Figure 9 shows the creep machine and laser extensometer used for the tests. Coupons measuring 600 mm x 38 mm x 9 mm were machined from the center of a 25,4 mm plate of AA7050-TAF.

Coupons were also tested in the creep machine without loads (σ=0) to evaluate the material behavior during the artificial aging. From solid solution to T7X aged temper condition, AA7050 presents three phase transformations (solid solution (σ)→GP zones→η'→η-$MgZn_2$)[16]. Once changes in the microstructure occur during the heat treatment and new phases appear it is important to know if the material will grow or shrink after aging in order to add or subtract these values from the creep curves obtained.

Figure 9. Creep machine and laser extensometer used for tests [Spirit Aerosystems].

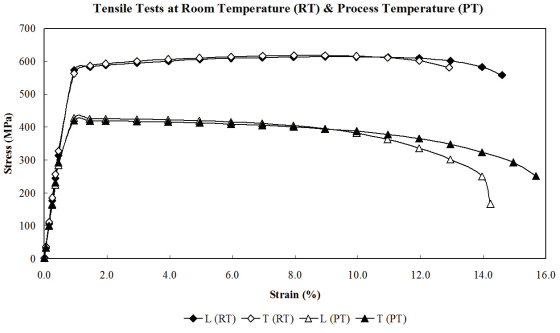

Figure 10. Tensile tests at room and process temperatures.

Table 2. Results from tensile tests.

Temperature	Rolling direction	σ_y (MPa)	E (GPa)
Room	L	581	68.90
Room	LT	571	70.90
Process	L	428	62.05
Process	LT	421	63.43

3. Results and Discussion

3.1. *Tensile tests*

Results from tensile tests are presented in Figure 10 and Table 2. Both σ_y and E were calculated graphically. At process temperature the values of σ_y and E are 26% and 10% (respectively) lower than that observed at room temperature.

Table 3. Values of initial stresses involved in CAF and the corresponding percentage of σ_y.

Temperature	Rolling direction	h (mm)	ε_T (%)	σ (MPa)	% σ_y
Process	L	10	0.313	194	45
Process	LT	10	0.313	198	47
Process	L	15	0.469	291	68
Process	LT	15	0.469	297	71

(a) (b)

Figure 11. Coupons after CAF: a) coupons and gage, b) deflection measurement.

Table 4. Force to push the coupon against the tool.

Rolling direction	E (GPa)	σ (MPa)	F (kN)
L	62.05	194	2.55
LT	63.43	198	2.60
L	62.05	291	3.82
LT	63.43	297	3.90

Table 5. Force from the autoclave over to coupon surface.

σ_a (MPa)	L (mm)	b (mm)	F (N)
0.7	400	70	19.600

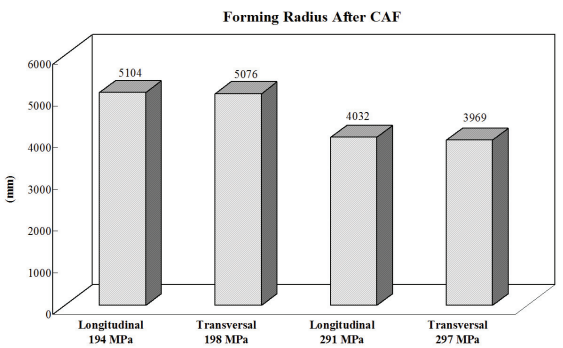

Figure 12. Forming radius after CAF.

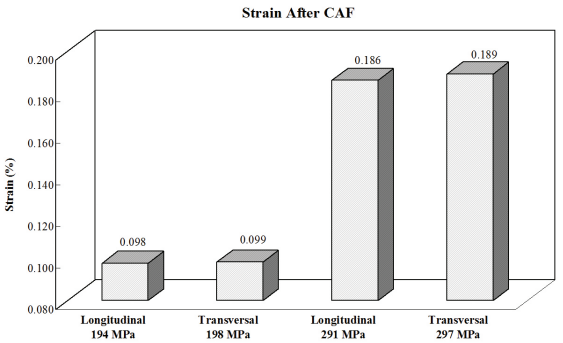

Figure 13. Residual strain after CAF.

3.2. *Creep age forming tests*

Using the values from Table 2 (σ_y and E) and Equations 1 to 3 it is possible to calculate the initial stresses. Despite the fact that the tensile tests were performed at room and process temperature, only the values for process temperature will be used because the total pressure is applied inside the autoclave only after the process temperature is reached.

Table 3 shows the initial stresses induced in the coupons during loading phase and the percentage of the material yield stress. Results from Table 3 confirm that CAF process runs under elastic stresses.

The force necessary to push the coupon against the tool was calculated using Equations 4 to 8 and the results are presented in Table 4.

Using the dimensions of coupons (L = 400 mm and b = 70 mm) and Equation 9 the resulting force from the autoclave can be calculated, as shown in Table 5.

Results from Table 5 confirm that the pressure inside the autoclave it is enough to push the coupon against the tool surface and then the initial stresses assumed before (190 MPa and 290 MPa) are correct.

Table 6. Results of the forming tests - adapted from[17].

Tool curvature (mm)		Average springback	
Span contour	**Chord contour**	**Span contour**	**Chord contour**
48000	1200	70	61
25000	800	60	58
10000	3000	54	65
8000	4000	55	67
8000	1300	55	51

Table 7. Effect of plate thickness on proof stress and springback - adapted from [9].

	2024A		8090		7449	
	10 mm	**25 mm**	**9 mm**	**25 mm**	**15 mm**	**25 mm**
0.2% PS, MPa	376	361	432	405	540	582
Springback, %	76	72	76	71	71	62

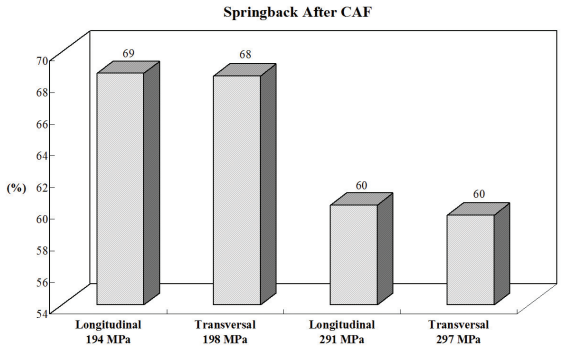

Figure 14. Spring back after CAF.

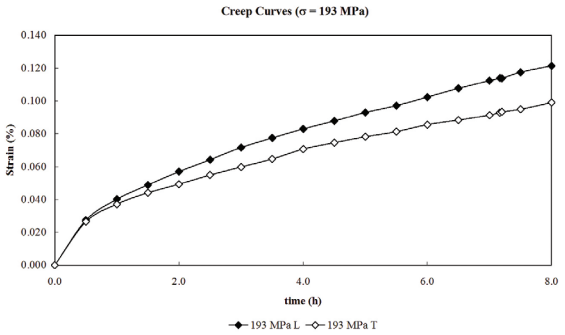

Figure 16. Creep curves at 193 MPa for AA7050-TAF (first and second stages observed),

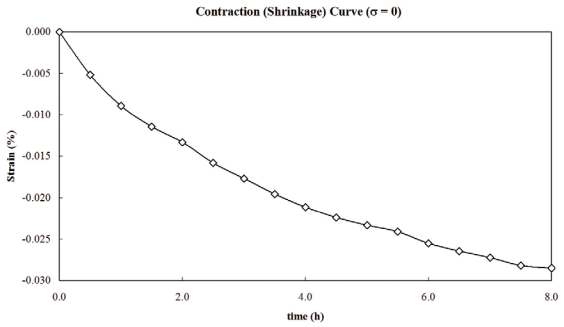

Figure 15. Contraction (shrinkage) curve for AA7050-TAF (creep test σ=0).

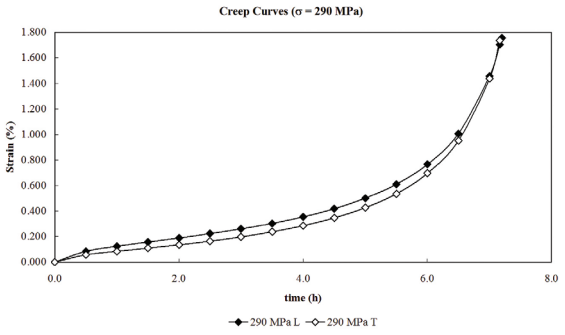

Figure 17. Creep curves at 290 MPa for AA7050-TAF (all three stages observed).

Figure 11 shows the coupons over a flat table where the deflections "f" were measured after CAF. Using the deflection values, the length of the coupons "L" and Equation 4 the forming radii "R_f" were calculated for every coupon. With the radii values, thickness "h" and Equation 5 the strain after CAF was calculated.

Results from forming radius and strain after CAF are shown in Figures 12 and 13. As expected the coupons with higher thickness results in lower forming radii - and higher strains after CAF - which means more forming. This fact can be explained because the initial stress induced in the thicker coupons is higher than the stress induced in the thinner coupons. and higher initial stress provides more stress relaxation during CAF.

As reported before [x], relaxation is proportional to initial stress. Moreover in the stress levels tested (190 MPa and 290 MPa) the predominant creep mechanism is dislocation creep which is very sensitive to stress.

Spring back after CAF was calculated using Equation 12. Coupons with thickness of 10 mm presented spring back

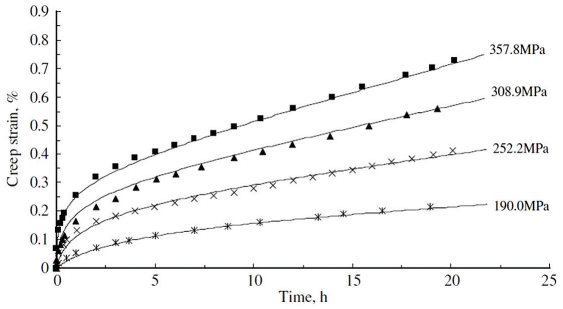

Figure 18. Comparison of experimental (symbols) and computed (solid curves) creep ageing curves for different stress levels - AA7055 at 120C - adapted from[18].

values around 68% while coupons with thickness of 15 mm presented spring back values around 60%. Figure 14 presents the results. These results are similar to that found in literature[9,17] as shown in Tables 6 and 7. In addition the results confirm that spring back is dependent on initial stress. Regarding the process time used for CAF, it can be said that the alloy 7050 in TAF condition presents good formability when processed by CAF in 8 hours.

3.3. *Creep tests*

Figure 15 presents the shrinkage or contraction curve of the AA7050 – TAF alloy which can be considered a creep test without load. The contraction observed is result of the artificial ageing that is part of CAF process. During heat treatment new phases precipitates and dimensional changes can take place. In the case of AA7050-TAF a total contraction of 0,028% is observed at the end of the test. This data shall be used to correct the creep curves in order to guarantee that only strain from creep will be evaluated.

Constant load creep tests in rolling direction (L) and perpendicular to rolling direction (LT) were performed at 193 MPa and 290 MPa. These stress values are the same observed in the loading phase of CAF tests. Figures 16 and 17 present the results.

First and second stages of creep can be noticed (for both directions) in the creep curves for the coupons tested at 193 MPa. Comparing the results it is observed that the coupon in L direction shows more creep strain than the coupon in LT direction (0.121% and 0.098%, respectively).

The results for coupons tested at 290 MPa are presented in Figure 17. Again, it is observed that the coupon in L direction shows more creep strain than the coupon in LT direction (1.750% and 1.737% respectively). However the creep curves for 290 MPa stress level presents all three stages and the coupon failed at 85% of the total time observed for the 193 MPa creep tests. This failure may indicate that initial stress of 290 MPa at process temperature can be a limitation for this alloy when submitted to CAF.

It is important to compare the results from creep tests with previous results. Zhan et al.[18] presented a set of curves for a similar alloy - AA7055 - in different stress levels, as shown in Figure 18.

The behavior of the two alloys (AA7050-TAF and AA7055) is similar for 190 MPa. The process time for creep tests based on AMS it is 8 hours. At this time, AA7050-TAF has a creep strain of 0.12% and AA7055 has a creep strain of 0.15% (coupons in rolling direction). On the other hand, for 290 MPa AA7050-TAF failure before the end of the test (creep strain around 1.7%) while AA7055 is in the second stage of creep (creep strain < 0.5%).

Two main reasons could explain the difference. First is the test temperature - 120°C for AA7055 and around 180°C for AA7050-TAF (according to AMS[15]). Higher temperature leads to higher creep strain. Secondly it is important to remember that TAF condition basically is the alloy with the first stage of the artificial aging complete which means that precipitates have already precipitated in the Al matrix. During CAF process the precipitates start to grow and become a barrier for dislocations movements and thus the strength of AA7050-TAF is higher than AA7055 that was tested from its solid solution condition - the precipitates have to nucleate and then will grow increasing the alloy strength.

4. Conclusions

Based on the results obtained in this experimental investigation, the following conclusions can be presented:

- Spring back after CAF is dependent on the initial stress, being lower as higher the initial stress;
- Values of spring back and forming radius after CAF are compatible with results found in literature for similar alloys even using lower soaking time;
- Creep strain of coupons tested at 193 MPa is compatible to other 7XXX alloys; however; for coupons tested at 290 MPa the alloy presented higher values of creep strain if compared to other 7XXX alloys which lead to the failure of the coupon;
- The alloy 7050 in TAF condition can be used for CAF since the initial stress is lower than 70% σ_y (290 MPa);
- Using the alloy 7050 in TAF condition allows CAF to be done in 8 hours which reduces manufacturing time and cost.

Considering the comments above it can be concluded that the use of AA7050 in TAF condition for CAF is feasible for the tests conditions presented in this work.

References

1. Ho KC, Lin J and Dean TA. Constitutive modelling of primary creep for age forming an aluminium alloy. *Journal of Materials Processing Technology.* 2004; 153-154:122-127. http://dx.doi.org/10.1016/j.jmatprotec.2004.04.304
2. Jeunechamps PP, Ho KC, Lin J, Ponthot JP and Dean TA. A closed form technique to predict springback in creep age-forming. *International Journal of Mechanical Sciences.* 2006; 48(6):621-629. http://dx.doi.org/10.1016/j.ijmecsci.2006.01.005
3. Eberl F, Gardiner S, Campanile G, Surdon G, Venmans M and Prangnell P. Ageformable panels for commercial aircraft. *Jounal of Aerospace Engineering.* 2008; 222(6):873-886.
4. Holman MC. Autoclave age forming large aluminum aircraft panels. *Journal of Mechanical Working*

Technology. 1989; 20:477-88. http://dx.doi.org/10.1016/0378-3804(89)90055-7

5. Zhan L, Lin J and Dean TA. A review of the development of creep age forming: experimentation, modeling and applications. *International Journal of Machine Tools & Manufacture.* 2011; 51(1):1-17. http://dx.doi.org/10.1016/j.ijmachtools.2010.08.007
6. Inforzato DJ, Costa Junior PR, Fernandez FF and Travessa DN. Creep-age forming of AA7475 aluminum panels for aircraft lower wing skin application. *Materials Research*. 2012; 15(4):596-602. http://dx.doi.org/10.1590/S1516-14392012005000080
7. Ho K.C, Lin J, Dean T.A, *Modelling of springback in creep forming thick aluminum sheets*, International Journal of Plasticity 20 (2004) 733–751.
8. Zhu A.W., Starke Jr E.A., *Material aspects of age-forming of Al_x-Cu alloys*, Journal of Materials Processing Technology, 117, (2001), 354 – 358.
9. Pitcher P.D., Styles C.M., *Creep Age Forming of 2024A, 8090 and 7449 Alloys*, Materials Science Forum, v. 331-337 (2000) pp 455-460.
10. Robey R.F., Prangnell P.B., Dif R., *A Comparison of the Stress Relaxation Behaviour of Three Aluminium Aerospace Alloys for use in Age-Forming Applications*, Materials Forum, v. 28, pág 132-138, 2004.
11. Zhan L, Lin J and Huang M. Constitutive modelling and springback prediction in creep age forming of AA7055 doubly curved panels. In: *Proceedings of the 14th International ESAFORM Conference on Material Forming*; 2011; Belfast, United Kingdom. Melville: American Institute of Physics; 2011. p. 235-240. (AIP Conference Proceedings, v. 1353).
12. Bakavos D, Prangnell PB, Bes B, Eberl F and Gardiner S. Through thickness microstructural gradients in 7475 and 2022 creep ageformed bend coupons. *Materials Science Forum.* 2006; 519-521:407-412. http://dx.doi.org/10.4028/www.scientific.net/MSF.519-521.407
13. Aerospace Material Specification – AMS. *AMS2770 Heat Treatment of Wrought Aluminum Alloy Parts.* AMS; 2011.
14. Aerospace Material Specification – AMS. *AMS4050 Aluminum Alloy, Plate 6.2Zn - 2.3Cu - 2.2Mg - 0.12Zr (7050-T7451) Solution Heat Treated, Stress Relieved, and Overaged.* AMS; 2011.
15. American Society for Testing and Materials – ASTM. *E8*: Standard Test Methods for Tension Testing of Metallic Materials. West Conshohocken: ASTM Internacional; 2011.
16. Berg LK, Gjonnes J, Hansen V, Li XZ, Knutson-Wedel M, Waterloo G et al. GP-Zones in Al–Zn–Mg alloys and their role in artificial aging. *Acta materialia*. 2001; 49(17):3443-3451. http://dx.doi.org/10.1016/S1359-6454(01)00251-8
17. Adachi T, Kimura S, Nagayama T, Takehisa H and Shimanuki M. Age forming technology for aircraft wing skin. *Materials Forum.* 2004; 28:202-207.
18. Zhan L, Lin J, Dean TA and Huang M. Experimental studies and constitutive modelling of the hardening of aluminium alloy 7055 under creep age forming conditions. *International Journal of Mechanical Sciences.* 2011; 53(8):595-605. http://dx.doi.org/10.1016/j.ijmecsci.2011.05.006